



Developing GEP tree-based, neuro-swarm, and whale optimization models for evaluation of bearing capacity of concrete-filled steel tube columns

Payam Sarir¹ · Jun Chen¹ · Panagiotis G. Asteris² · Danial Jahed Armaghani³ · M. M. Tahir⁴

Received: 2 May 2019 / Accepted: 18 June 2019 / Published online: 25 June 2019
© Springer-Verlag London Ltd., part of Springer Nature 2019

Abstract

The type of materials used in designing and constructing structures significantly affects the way the structures behave. The performance of concrete and steel, which are used as a composite in columns, has a considerable effect upon the structure behavior under different loading conditions. In this paper, several advanced methods were applied and developed to predict the bearing capacity of the concrete-filled steel tube (CFST) columns in two phases of prediction and optimization. In the prediction phase, bearing capacity values of CFST columns were estimated through developing gene expression programming (GEP)-based tree equation; then, the results were compared with the results obtained from a hybrid model of artificial neural network (ANN) and particle swarm optimization (PSO). In the modeling process, the outer diameter, concrete compressive strength, tensile yield stress of the steel column, thickness of steel cover, and the length of the samples were considered as the model inputs. After a series of analyses, the best predictive models were selected based on the coefficient of determination (R^2) results. R^2 values of 0.928 and 0.939 for training and testing datasets of the selected GEP-based tree equation, respectively, demonstrated that GEP was able to provide higher performance capacity compared to PSO–ANN model with R^2 values of 0.910 and 0.904 and ANN with R^2 values of 0.895 and 0.881. In the optimization phase, whale optimization algorithm (WOA), which has not yet been applied in structural engineering, was selected and developed to maximize the results of the bearing capacity. Based on the obtained results, WOA, by increasing bearing capacity to 23436.63 kN, was able to maximize significantly the bearing capacity of CFST columns.

Keywords The concrete-filled steel tube columns · Bearing capacity · GEP-based tree · Neuro-swarm · WOA · Optimization

1 Introduction

In the area of structural performance, one of the key issues is how to use the available materials in an optimized way. In current construction processes, the two most widely used materials are steel and concrete. They can be used together in such a way that each one of them can improve the other's performance, which finally results in a better overall behavior of the structure under various loads. As a result, when concrete and steel are combined appropriately, their

performance will be more improved compared to the cases where they are utilized separately. Recently, composite material has been widely applied to different construction projects [1, 2] as well as to retrofitting and rehabilitation purposes [3, 4] across the world. Composite columns offer many benefits; they can be easily produced, they enjoy some improved features compared to other columns such as steel structures, and they reduce the construction expenses [1].

Accordingly, several researchers have attempted to test how the concrete-filled hollow steel columns behave in different conditions [5–8]. Based on the findings of the study conducted by He et al. [9], among different types of composite columns, the concrete-filled steel tube (CFST) can outperform the other types of columns. The concrete in CFST is employed inside, while the steel's hollow sections are in the surrounding periphery. It helps the steel column not to be suddenly buckled, improves the way it performs, and delays

✉ Jun Chen
chen_jun@sjtu.edu.cn

✉ Danial Jahed Armaghani
danialarmaghani@gmail.com

Extended author information available on the last page of the article

the settlement because of the external loads. When these columns are being designed, a key issue is to examine the interactive impacts that occur between steel and concrete. This issue has not been investigated adequately in literature. Although there are some studies carried out into composite columns on the basis of experiments and theories, in most of the cases (e.g., [8]), the authors have not sufficiently described the columns' behaviors under a variety of loading conditions.

In recent years, the civil engineering field has witnessed the advance of numerous methods. One of the most significant methods is soft computing and intelligent technique [10–30]. Such techniques are presented in a variety of models in various sections of engineering [31]. For example, artificial intelligence is used in civil engineering for prediction and optimization purposes, e.g., the prediction of the concrete's compressive strength [20, 29–40], the identification of the risk areas of regional transportation corridors [41], the prediction of final strength of reinforce concrete beams with fiber-reinforced plastic (FRP) strengthened in shear [8], the determination of damage in skeletal structure [42], and the optimization of the arch dam forms [43].

To improve the precision level in the computation of the parameters, the artificial neural network (ANN) can be effectively used [12–15, 27, 41]. Even though ANNs have dynamic research realms in science and engineering, directly map the input to output patterns, and are able to use all effective prediction characteristics, they have limitations such as slow learning rate and entrapment in local minima [44]. The use of optimization techniques such as particle swarm optimization (PSO) in different engineering optimized affairs can address the shortcomings of ANN. In fact, PSO is able to optimize weights and biases of ANN to get better performance prediction.

In the engineering field, a recently introduced technique called gene expression programming (GEP) has been found successful in enhancing the accuracy level. It is actually a combined form of genetic algorithm (GA) and genetic programming (GP). It has shown a high capability of introducing mathematical equations to do the predictions with a higher quality and solving problems of a high complexity [45, 46]. Lots of studies have reported the success of GEP in different fields of civil engineering, including the environmental issues of blasting [47, 48], piling [49], tunneling and rock mechanics [50, 51], concrete technology [52, 53], highway construction [54], and river engineering [55, 56].

The present study is aimed to propose efficient models based on these artificial intelligence approaches in order to predict the axial load bearing capacity of the composite columns. To this end, experimental data are gathered and required tests are carried out on parameters that affect the bearing capacity of columns. Next, the gathered data are applied to the formation and development of various models

of GEP. Then, a comparison is made between the results of the proposed model and those of hybrid PSO–ANN (or neuro-swarm) and ANN networks. At the final step, to achieve the optimum cross-sections, a whale optimization algorithm (WOA), which is considered as a novel optimization algorithm, is proposed. In the following, the theoretical underpinning of the models used in this study is explained first, the datasets are described, and the prediction phase of the study is then discussed. To achieve the optimum values of the variables, the best predictive model will be selected and then it will be utilized as an input model in the WOA optimization technique.

2 Predictive model background

2.1 Artificial neural network (ANN)

The concept of neural networks was first introduced in 1950s by Donald Hebb [57] with the introduction of a simple learning mechanism. He developed this method by investigating human brain neurons and the effect of learning on them. In each neuron of ANN, dendrites receive information from the previous neuron, and axons transfer the results to the next section (i.e., next neuron) after an initial processing. Chemical signaling is done through synapses between the cells. The performance of a computational neuron, which is used in neural networks, is similar (assuming sigmoid activation function) to that of a biological neuron with inputs and outputs. An ANN contains two or more layers, and each layer has a series of neurons. The strength of the links between the layers is associated with the weights constituting a network. The weights associated with each neuron linearly transform the input vectors, which become the arguments of each neuron's non-linear activation function (transfer function). Two main algorithms, i.e., feed-forward multilayer and back-propagation (BP), are used in neural networks. BP is more common and recommended by different researchers [58–60]. This algorithm updates the weights in order for the loss functions to reach the minimum error (loss) in the system. This training process is repeated for a few times so that it can reach the termination criterion. The BP phrase is associated with conditions in which gradient is calculated for non-linear multilayer networks (the networks that are used to solve most of the engineering problems). The sigmoid transfer function receives the input values and presents them as an interval of 0–1, regardless of the initial input interval [61–64].

2.2 Particle swarm optimization (PSO)

Kennedy and Eberhart [65] introduced a solution for optimal continuous problems called particle swarm optimization

(PSO). PSO is a non-linear procedure inspired by social systems such as fish shoals. Indeed, PSO has been formed based on the number of particles, which is established randomly. Seeking an optimal value goal is another PSO stage as an iterative process. In this stage, the particles are adjusted to their positions based on their own experience and that of other particles. To gain the best position, each particle follows its own best position (P_{BEST}) and global best position (G_{BEST}) among other particles. Moreover, each particle tends to move toward its own P_{BEST} and G_{BEST} during the training process based on a new velocity term and distance of its best positions in the learning stage. Respectively, the new position of each particle depends on the new velocity value in next iteration [66, 67]. In PSO, Eqs. (1) and (2) are used to gain the velocity updated and movement. Equation (1) calculates the particle’s real movement through its velocity vector and Eq. (2) adjusts the vector to the P_{BEST} and G_{BEST} .

$$\vec{v}_{new} = \vec{v} + C_1 \times (\overline{pbest} - \vec{p}) + C_2 \times (\overline{gbest} - \vec{p}) \quad (1)$$

$$\vec{p}_{new} = \vec{p} + \vec{v}_{new} \quad (2)$$

where \vec{v}_{new} is the new particle velocity, \vec{v} the current particle velocity, \vec{p}_{new} the new particle position, \vec{p} the current particle position, C_1 and C_2 are the coefficients, and \overline{pbest} and \overline{gbest} are the personal and global positions of particles, respectively.

The flowchart of PSO is shown in Fig. 1. More details about PSO and its structure are available in the literature [68].

2.3 Gene expression programming (GEP)

To explain more, GEP is known as one of the innovative methods developed in the field of artificial intelligence. It is actually a developed version of GA and GP. GEP, comprising various parts, suggests appropriate solutions to a variety of problems [69]. It uses two main chromosomes, and the expression tree used in this algorithm shows capacity for removal of the limitations of the two antecedents (GA and GP). In GEP, codifications are normally presented in the shape of a string attained from the Karva programming language; it is able to behave similar to ETs. Interestingly, GEP is capable of presenting its own models by means of mathematical equations that, in turn, form relationships between dependent and independent parameters. In the context of the engineering field, it is of a high importance and practicality to create models with the capacity of providing equations. Such methods are efficient substitutes for the ANN models in solving the problems. These issues have led the scholars in this field to further develop such methods.

In GP, a variety of mathematical functions, including $-$, $+$, \times , \sin , etc., are noted and applied to the variables; thus, a

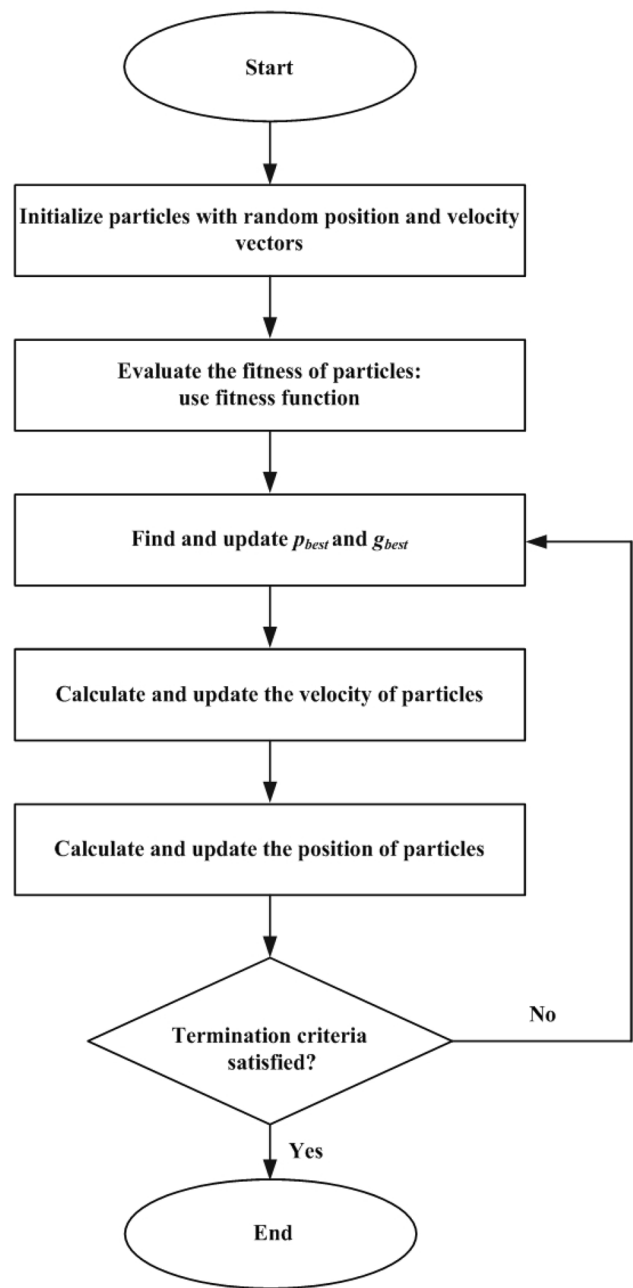
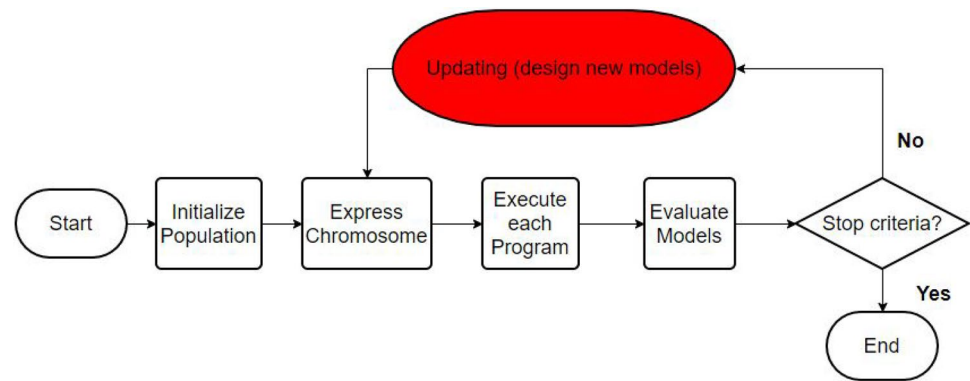


Fig. 1 The flowchart of PSO algorithm [65]

mathematical set is obtainable through combining them for the purpose of problem examination. In chromosomes with more than one gene, each gene denotes a sub-ET comprising a head and a tail. Such symbolic chromosomes need to be defined as trees of various forms and sizes (expression trees). According to Fig. 2, the GEP modeling process begins with the random creation of chromosomes for determined numbers, which follows Karva language (Karva is a symbolic language to introduce chromosomes). These points are tested considering the functions that control the models and

Fig. 2 A view of GEP system



their adaptability level. Such functions are of various types each of which can be defined using a variety of criteria. The functions include root relative squared error (RRSE), mean absolute error (MAE), and root mean square error (RMSE). In the next step, in case of not satisfying the termination criterion (that is the achievement of the maximum iteration or the proper fitness value), the best chromosomes chosen by means of the Roulette Wheel method for the first process will enter the next structure. Then, the most important genetic operators, namely mutation, transfer (RIS, IS, and gene transfer), and reconstruction (one point, two points, and gene reconstruction), will be applied to existing chromosomes in accordance with their proportions, which can be defined using the codes and the experts' opinions of the GP method. This way, new chromosomes replace the remains, and the process continues until the termination criteria are fully satisfied [70–72]. Literature consists of more detailed information regarding GEP and the way it can be implemented initially [73].

2.4 Whale optimization algorithm (WOA)

The whale optimization algorithm (WOA) was proposed in 2016, mimicking the hunting mechanism of humpback whales in nature [74]. The most interesting thing about the humpback whales is their special hunting method. This foraging behavior is called bubble-net feeding method [75]. Humpback whales prefer to hunt school of krill or small fish close to the surface. It has been observed that this foraging is done by creating distinctive bubbles along a circle or a '9'-shaped path as shown in Fig. 3. The three-dimensional hunting behavior was studied in 2011; before that, the hunting behavior was studied based on observation from the sea surface. Nevertheless, Goldbogen et al. [76] conducted a different investigation based on the use of tag sensors. In this new method of study, they captured 300 tag-derived bubble-net feeding events of 9 individual humpback whales and introduced two new bubble movement plans, i.e., upward spirals and double loops. In the previous movement plan, humpback whales create bubble from depth of around 12 m

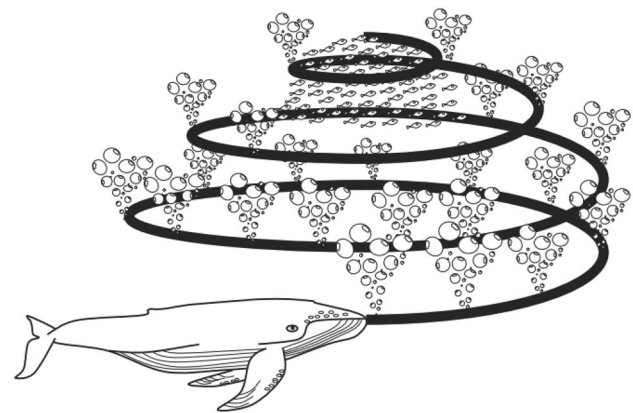


Fig. 3 The behavior of humpback whales in WOA designing process [74]

in a spiral shape around the prey and swim up toward the surface. However, the new movement plan found by Goldbogen et al. [76] consisted of three different stages: coral loop, lobtail, and capture loop [76]. It is important to note that bubble-net feeding is a unique behavior that can only be observed in humpback whales. More details regarding WOA can be found in the original reference [74].

3 Established database

The CFST columns/structures, as noted earlier, have been implemented in the main lateral resistance systems of both braced and unbraced building constructions. Moreover, this type of columns has been widely recommended for the retrofitting projects to improve the columns bearing capacity, particularly when situated in dynamic conditions. As a result, it is of a high importance to appropriately predict the CFST bearing capacity. To this end, a database containing totally 303 test results was taken into consideration for the purpose of this study. The data, which were on the basis of wide-ranging laboratory experiments, were gathered from

the literature [9, 77–83]. In the following, the testing procedure used in this study is simply explained.

During the concrete casting process carried out in laboratory using formworks, a support system was created, which included steel bars, wooden plates, European pallet, and bottom steel blocks. It was used for the purpose of ensuring the steel tube stability in the course of casting the concrete. The top surface of the outer steel tube was approximately 25 mm higher than the top surface of the inner concrete core. Following the casting operation, all of the composite columns and cylinder specimens for reference tests were cured at room temperature within the laboratory conditions. Prior to the start of testing process, the steel tube (L) and overall length of the concrete core (L_c) were precisely determined. At both ends of the concrete core, two steel blocks were positioned in a way to apply the axial load upon the concrete core. After that, we made use of the servo-controlled hydraulic testing system to compress concentrically the prepared specimens. A load cell was employed to record the applied force. Then, with the rate of 0.01 mm/s, the axial load was amplified upon the columns in a gradual manner, and simultaneously, the axial displacement was measured using the linear varying displacement transducers (LVDTs). This process went on until the measured axial displacements were roughly 20 mm. Next, the maximum axial compressive strength of the columns, i.e., their bearing capacity, was obtained as output of the study.

In case of all gathered datasets, to predict the bearing capacity of CFST columns (P_{exp}), five parameters were taken into account as input parameters; they were the concrete compressive strength (f_c), the column length (L), outer diameter (D), tensile yield stress of the steel column (f_y), and steel cover thickness (t). This is worth noting that ranges of (23.2–188.1 MPa), (60–450 mm), (180–4000 mm), (0.86–10.37 mm), (185.7–853 MPa), and (215–13,776 kN) were considered for concrete compressive strength, outer diameter, length of column, steel cover thickness, tensile yield stress of the steel column, and bearing capacity of CFST columns, respectively. Table 1 shows 100 items of data (as examples) out of 303 data used in the modeling of this study. In addition, distributions of the data are displayed in Figs. 4, 5, 6, 7, 8, and 9. In addition, the flowchart of this paper with details is shown in Fig. 10.

4 Prediction modeling

4.1 ANN modeling

As the previous sections mentioned, ANN is capable of suggesting proper solutions to both linear and non-linear engineering problems. This section presents the neural network models in such a way that their obtained results could be

compared with those of the PSO–ANN and the new GEP models discussed in the following subsections. For the purpose of designing the required networks, 80% of all data (i.e., 242 cases) were allocated to the training section in order to be applied to the development process of the models and the remaining 20% were assigned to the testing section to make required evaluations on the model developments [84–88]. Such categorization helps to effectively assess the performance of artificial models regarding the prediction of the CFST columns bearing capacity.

Generally, a key criterion applied to designing of ANN is RMSE; it is considered as the initial termination criterion of the network training process. The RMSE value is obtainable using the values coming from the system (network) and the measured values. Remember that when $RMSE = 0$, the most appropriate model is achieved.

$$\Delta = t - E_{st}, \quad (3)$$

$$RMSE = \sqrt{\text{Average} \left[\sum_{k=1}^{NT} \Delta_k^2 \right]}. \quad (4)$$

The parameters E_{st} , t , Δ , and k stand for the measured values, predicted values, error, and number of network outputs, respectively. Furthermore, the determination coefficient (R^2) value was also employed; it was responsible for determining the correlation between the measured value and the predicted one. When $R^2 = 1$, it is in its best condition. The two criteria of R^2 and RMSE were applied to the evaluation of the prediction models proposed in the present study. We took into consideration different explanations provided in the related literature; then, various ANN models were designed and configured in a way to be effectively used for the prediction of the CFST columns bearing capacity. Figures 11 and 12 present the models of this method for training and testing sections, respectively. As it is clearly observable, the most proper performance of the model was achieved when the iteration value was fixed at 250 and the number of neuron was set to 8. More required details in regard to the most appropriate ANN model for the prediction of bearing capacity of the CFST columns will be presented later.

4.2 PSO–ANN modeling

ANNs have been developed through applying optimization algorithms like GA and PSO for solving engineering problems [26, 61, 89–92]. Regarding BP as a local seeking learning algorithm, the optimal seeking procedure of ANN might be failed with unfavorable solution. Therefore, PSO could be used to adjust the biases and weights of ANN in its performance developing. Considering the local minimal of ANN, there would be occasionally high possibility of convergence; however, PSO has the capability of finding a

Table 1 100 data out of 303 data used in this research

Dataset number	f'_c (MPa)	D (mm)	L (mm)	t (mm)	f_y (MPa)	P_{exp} (kN)
1	77.1	165	571	2.82	363.3	2608
2	77.1	190	656	1.94	256.4	3083
3	77.1	190	658	1.52	306.1	2830
4	77.1	190	662.5	1.13	185.7	2630
5	108	190	661.5	1.13	185.7	3220
6	77.1	190	664	0.86	210.7	2553
7	40	160.1	2000	4.98	280	1261
8	41	160.2	2500	4.96	281	1244
9	43	160.3	3000	5	270	1236
10	41	160.2	3500	4.97	273	1193
11	45	159.9	4000	4.98	281	1091
12	70	159.8	2000	5.01	283	1650
13	71	159.7	2500	5.2	281	1562
14	73	159.8	3000	5.1	276	1468
15	74	160.1	3500	4.98	276	1326
16	71	160.2	4000	5.02	281	1231
17	99	160.3	2000	5.03	281	2000
18	100	159.8	2500	5.01	275	1818
19	101	159.7	3000	4.97	275	1636
20	106	159.6	3500	4.98	270	1454
21	102	159.8	4000	4.97	270	1333
22	42.2	133	1862	4.5	325	882
23	42.2	133	1862	4.5	325	715
24	42.2	133	2793	4.5	325	784
25	42.2	133	2730	4.5	325	282
26	42.2	133	2730	4.5	325	268
27	31.4	114.43	300	3.98	343	948
28	93.6	114.57	300	3.99	343	1308
29	34.7	114.43	300	3.82	343	929
30	97.2	114.26	300	3.93	343	1359
31	34.7	114.88	300.5	4.91	365	1380
32	104.9	115.04	300	4.92	365	1787
33	57.6	115.02	300.5	5.02	365	1413
34	57.6	114.49	299.3	3.75	343	1038
35	57.6	114.29	300	3.75	343	1067
36	31.9	114.3	300	3.85	343	998
37	31.9	114.09	300.5	3.85	343	948
38	98.9	114.54	300	3.84	343	1359
39	98.9	114.37	299.5	3.85	343	1182
40	48.3	165	562.5	2.82	363.3	1759
41	38.2	165	571	2.82	363.3	1649
42	38.2	190	659.5	1.94	256.4	1652
43	48.3	190	658	1.52	306.1	1841
44	38.2	190	657	1.13	185.7	1308
45	38.2	190	657.5	0.86	210.7	1240
46	56.4	165	581	2.82	363.3	2040
47	56.4	190	655.5	1.94	256.4	2338
48	80.2	190	658.5	1.52	306.1	2870
49	56.4	190	661.5	1.13	185.7	1862
50	158.46	189	756	3	398	4837
51	165.49	168.6	648	3.9	363	4216

Table 1 (continued)

Dataset number	f'_c (MPa)	D (mm)	L (mm)	t (mm)	f_y (MPa)	P_{exp} (kN)
52	167.87	169	645	4.8	399	4330
53	158.75	168.7	645	5.2	405	4751
54	151.91	168.8	650	5.7	452	4930
55	158.75	168.1	645	8.1	409	5254
56	67.94	165	500	2.81	350	2160
57	67.94	165	500	2.76	350	2250
58	31.75	114.3	342.9	3.35	287.33	816.2
59	56.99	114.3	342.9	3.35	287.33	995.7
60	86.21	114.3	342.9	3.35	287.33	1242.2
61	102.43	114.3	342.9	3.35	287.33	1610.6
62	31.75	114.3	342.9	6	342.95	1380
63	56.99	114.3	342.9	6	342.95	1425.3
64	86.21	114.3	342.9	6	342.95	1673.9
65	102.43	114.3	342.9	6	342.95	1943.4
66	43.92	108	324	4	336	1235
67	164.35	114.3	200	6.3	428	2866
68	164.35	114.3	200	6.3	428	2595
69	29.5	165.2	200	3.7	366	1428.32
70	43.5	165.2	200	3.7	366	1676.42
71	58	165.2	200	3.7	366	2094.15
72	81.6	165.2	200	3.7	366	2511.3
73	29.5	165.2	200	3.7	366	1630.56
74	43.5	165.2	200	3.7	366	1737.94
75	42.2	133	465	4.5	325	576
76	37.5	240	720	1.48	307	2300
77	37.5	240	720	1.48	307	2150
78	31.7	114.3	342.9	3.35	287.3	816.2
79	57	114.3	342.9	3.35	287.3	995.7
80	31.7	114.3	342.9	6	343	1380
81	57	114.3	342.9	6	343	1425.3
82	23.2	101.6	304.8	3.03	371	635
83	23.2	101.8	305.4	3.03	371	679
84	23.2	101.8	305.4	3.03	371	632
85	24.3	216.5	649.5	6.61	452	3568
86	24.2	318.5	955.5	10.37	335	6901
87	40.2	101.6	304.8	3.03	371	864
88	40.2	101.7	305.1	3.03	371	803
89	38.2	216.5	649.5	6.61	452	4200
90	39.2	318.4	955.2	10.37	335	7742
91	51.3	101.5	304.5	3.03	371	859
92	51.3	101.9	305.7	3.03	371	926
93	46.7	216.4	649.2	6.61	452	4283
94	52.2	318.3	954.9	10.37	335	9297
95	36.2	168.6	645	3.9	363	1771
96	80.2	190	658.5	1.52	306.1	2870
97	74.7	190	657.5	0.86	210.7	2433
98	77.1	165	571	2.82	363.3	2608
99	77.1	190	656	1.94	256.4	3083
100	77.1	190	658	1.52	306.1	2830

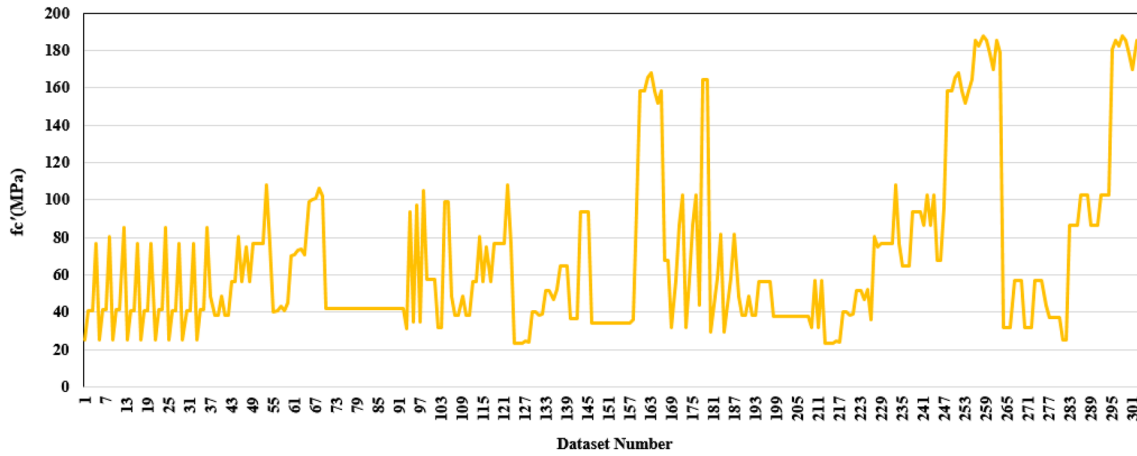


Fig. 4 Statistical distribution of concrete compressive strength

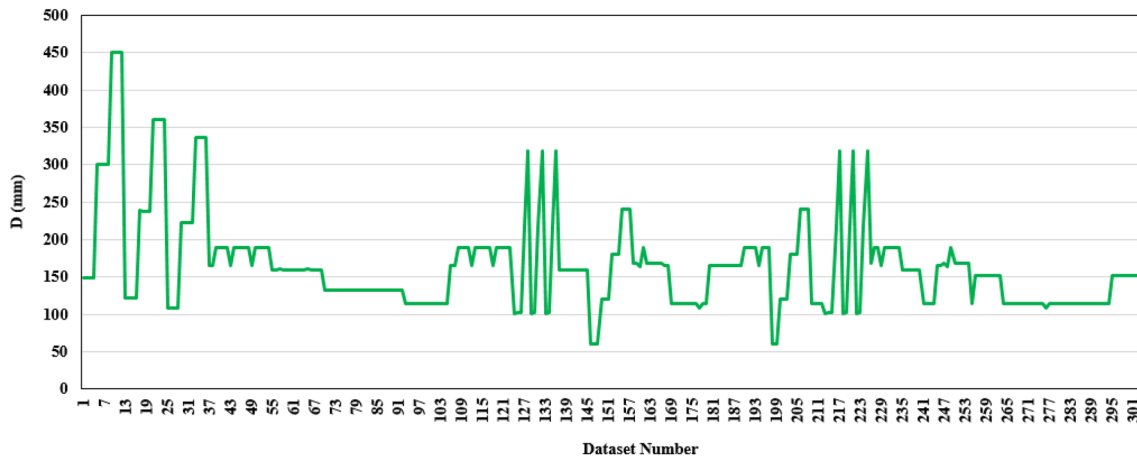


Fig. 5 Statistical distribution of outer diameter

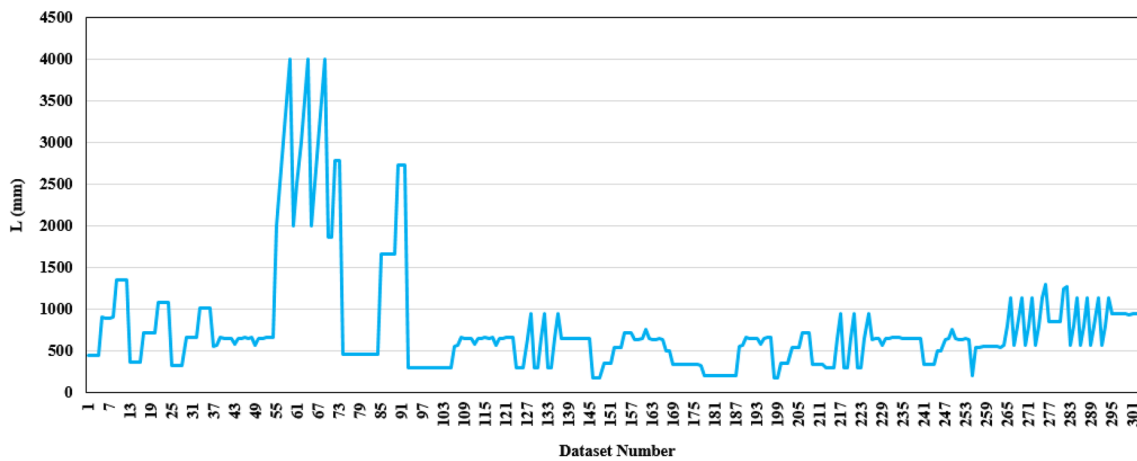


Fig. 6 Statistical distribution of length of column

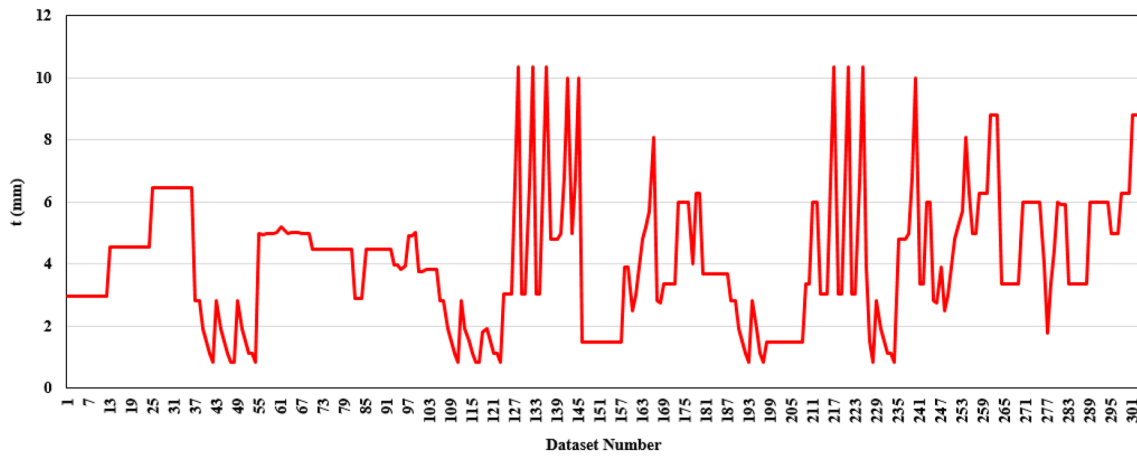


Fig. 7 Statistical distribution of steel cover thickness

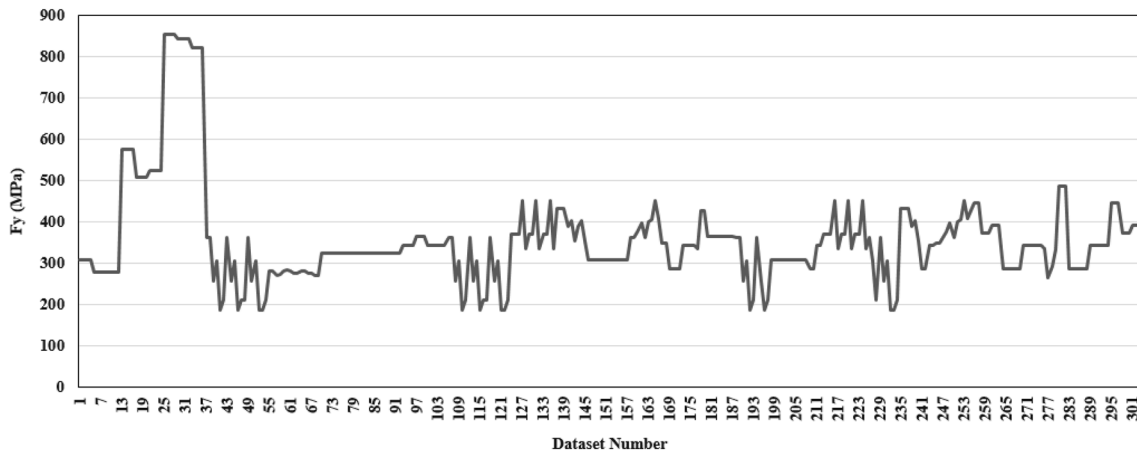


Fig. 8 Statistical distribution of tensile yield stress of the steel column

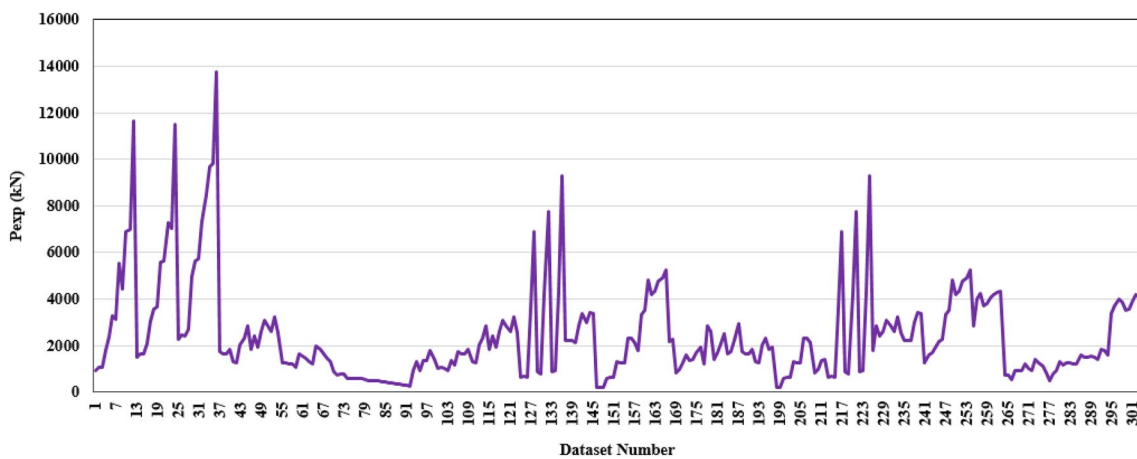


Fig. 9 Statistical distribution of bearing capacity of CFST columns

Fig. 10 Flowchart of this study

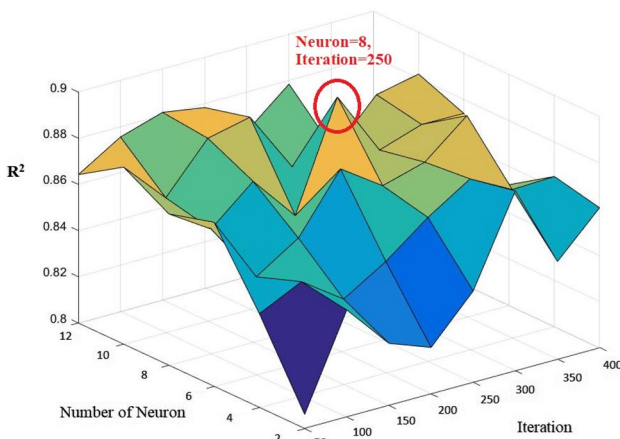
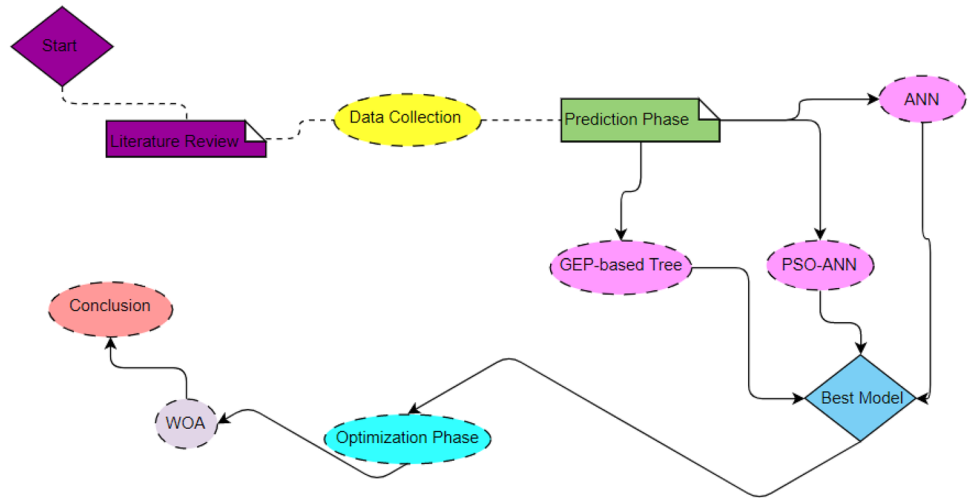


Fig. 11 Performance of ANN model for training datasets

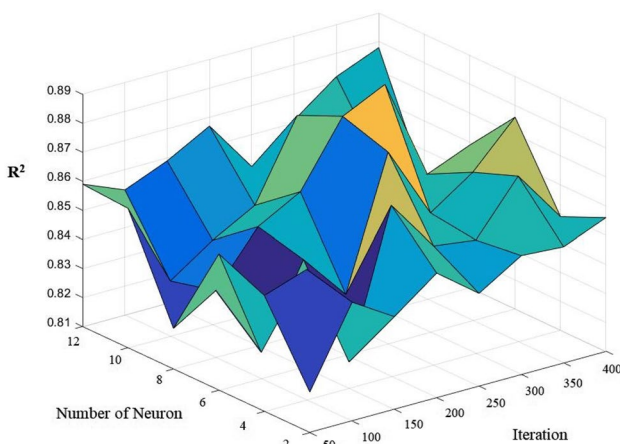


Fig. 12 Performance of ANN model for testing datasets

global minimum. Thus, PSO–ANN would enjoy the search characteristics of their technique. Regarding the search space, PSO searches the global minimum and the ANN will use them to find the best performance with lowest system error.

As previously mentioned, there would be few effective parameters on performance of PSO–ANN like swarm size, inertia weight, and coefficient velocity. According to Armaghani et al. [93], in this study, inertia weight, which is equal to 1 (among the other proposed values of 0.25, 0.5, and 0.75), was selected and applied in PSO–ANN model. Through a parametric research, different combinations of C_1 and C_2 were regarded to make PSO–ANN models. While, the best model based on the lowest system error was assigned to the combination of $C_1 = C_2 = 2$. Therefore, the variables are set as the best C_1 and C_2 in the PSO system. To determine the swarm size (SS) and the maximum number of iteration (I_{Max}), different SS values ranging from 50 to 400 with incremental step of 50 were taken into account with a total number of iteration = 500. Thus, eight PSO–ANN models were built to predict bearing capacity of CFST columns. Figure 13 displays the effects of SS and I_{Max} on performance prediction of PSO–ANN models. According to this figure, the lowest system error was gained by blue line or SS = 300, showing that a PSO–ANN model with SS = 300 is able to provide the highest performance capacity in predicting bearing capacity of CFST columns. On the other hand, RMSE values of SS were gradually reduced from iteration number 1 until iteration number 400. After iteration number 400, the RMSE results are constant with no alteration. As a result, in this paper, 400 was selected as I_{Max} to predict bearing capacity of CFST columns.

To sum up, inertia weight of 1, $C_1 = C_2 = 2$, $I_{Max} = 400$, SS = 300, and the number of hidden nodes = 8 were optimized as PSO and ANN parameters. It is important to mention that in modeling of PSO–ANN, the same architecture

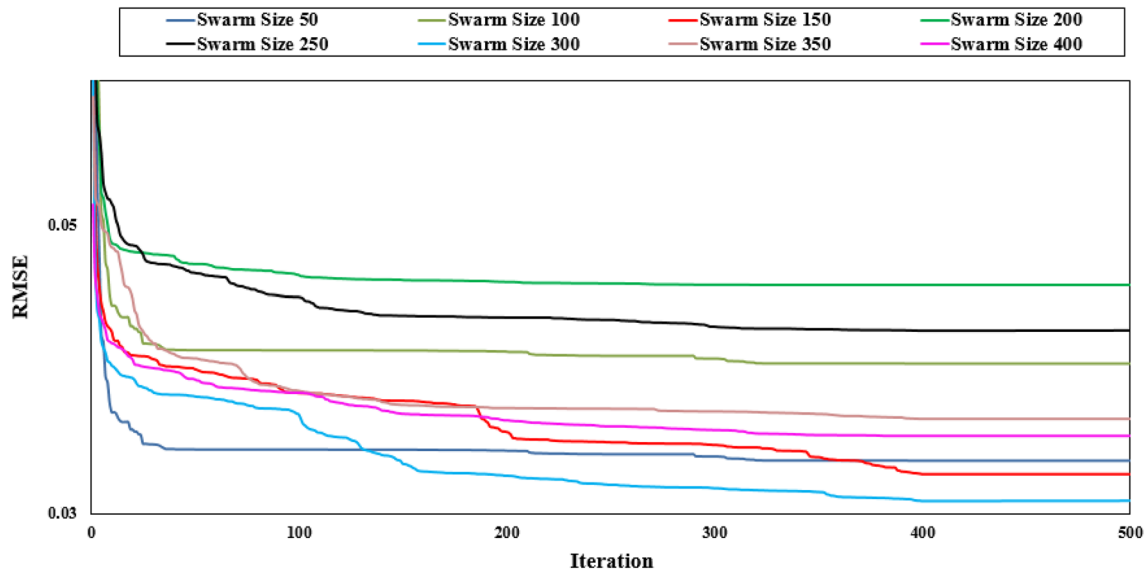


Fig. 13 The effect of I_{Max} and SS on performance of PSO–ANN model

obtained from ANN section was used. More discussion regarding the best PSO–ANN model in estimating bearing capacity of CFST columns will be given later.

4.2.1 GEP-based tree modeling

After obtaining the results of ANN and PSO–ANN networks, GEP predictive models are implemented in this stage, aiming at developing equation for predicting bearing capacity of CFST columns. The values and way of implementing them until obtaining the results of GEP models as well as presenting the relations will be all presented in the mathematical way. The process used in this research for implementing GEP is as follows:

1. In the first step, the fitness function was selected as a criterion for each chromosome’s merit occurrence. RMSE is the common fitness function that is used in modeling process of GEP. However, based on the problem’s conditions, different modes can be used for investigating the models’ performance more accurately. Therefore, each chromosomes’ fitness was determined as follows:

$$RMSE' = \frac{1}{1 + RMSE} \times 1000. \tag{5}$$

2. The second step was to allocate two important sections called the set of terminals (T) and functions (F) to the chromosomes’ structure, which created a mixture of them. The independent variables are considered as the terminal set, and the function set is usually defined according to the main core of the problem. In the current

study, trigonometry and mathematical functions were used as follows:

$$F = \{+, -, \times, \cdot, \text{Sin}, \text{Cos}, \text{ArcTan}, \text{tanh}, \text{sqrt}\} \tag{6}$$

3. In the third step, structural parameters of GEP were introduced and applied to the system. The number of genes parameter was introduced for ET subsections specified for each chromosome. According to Ferreira’s investigation [72, 73, 94] and some other researchers [79–83], the best way to obtain proper values for structural parameters of GEP is the method of trial and error. The analysis process started with the increasing values of the above-mentioned parameters of GEP, and then the predictive performance of the GEP model was checked. Several GEP models are designed and implemented with different parameters for predicting compressive strength of composite columns. Finally, after executing these processes for several times, values of the number

Table 2 GEP model parameters

Description of parameters	Value
Mutation rate	0.035
Inversion rate	0.1
IS transposition rate	0.1
RIS transposition rate	0.1
Gene transposition rate	0.3
One-point recombination rate	0.3
Two-point recombination rate	0.1
Gene recombination rate	0.1

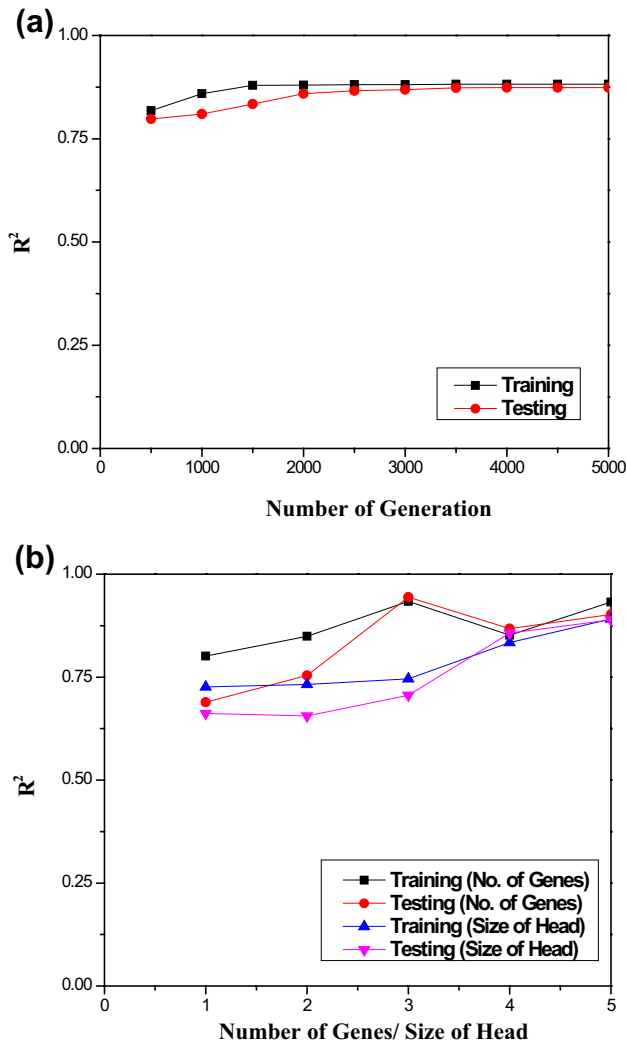


Fig. 14 Effects of the most influential parameters on GEP results: **a** number of generations, **b** number of genes/size of head

of chromosomes, head size, and number of genes were found to be 40, 5, and 3, respectively, for this section.

- Step 4 was to select the rates of genetic operators. In this step, assuming the proposed values by previous researchers [64, 65, 84], some other GEP models were created using the trial and error method. The obtained values of GEP parameters are tabulated in Table 2.
- In the final step, the linking function for connecting the created genes was defined. There are various linking functions like addition (+), subtraction (-), division (\div), and multiplication (\times). In this research, addition of different sections was used to connect sub-ETs because it provides a better connection in comparison with other functions.

To evaluate the predictive performance of the GEP models, R^2 and RMSE were used as performance indices. Several parameters of the GEP model were examined in this

Table 3 The equations to predict the bearing capacity of CFST columns with GEP

Model	Equations	R^2
1	$P \text{ exp} = ((d(1) \times \sqrt{d(4)}) - 133.82) + ((\frac{d(4)+d(2)}{\sqrt{d(0)}}) \times 36.666) + (((d(0) + d(2)) - 141.296) + (d(4) \times d(2)))$	0.9117
2	$P \text{ exp} = (((d(3) \times d(1)) + (d(3) \times d(1))) - 426.051) + (((-15.288 \times d(0)) + (d(4) - d(2))) - 233.753) + \sqrt{((13.491 - d(0) \times d(1)) \times (-8.065 \times d(1)))}$	0.9147
3	$P \text{ exp} = (d(4) \times (\sqrt{d(1)} + d(3) - 6.018)) + (((d(4) \times 7.509) - (7.509 - d(2))) \times \tanh(-3.36)) + (\sqrt{d(0)} \times (d(1) + d(1)) - (d(4) + d(4)))$	0.9147
4	$P \text{ exp} = (\sqrt{d(0)} \times (d(1) + d(1) - d(4) + d(4)) + (d(4) \times (\sqrt{d(1)} - (6.219 - d(3)))) + (\frac{d(4) \times 8.078 - d(2) \times (-0.626)}{\tanh(-2.831)})$	0.9277
5	$P \text{ exp} = (((\frac{d(1)}{1.231}) \times (\frac{d(0)}{9.248})) - d(2)) + (((3.925 + d(0)) - (d(4) + d(3))) \times (7.778 - d(3))) + (((\sqrt{d(4)} - \frac{d(3)}{-5.198})) \times d(1))$	0.9088

$d(0) = f'_c$ (MPa), $d(1) = D$ (mm), $d(2) = L$ (mm), $d(3) = t$ (mm), $d(4) = f_y$ (MPa)

Fig. 15 The tree expression of Eq. (4)

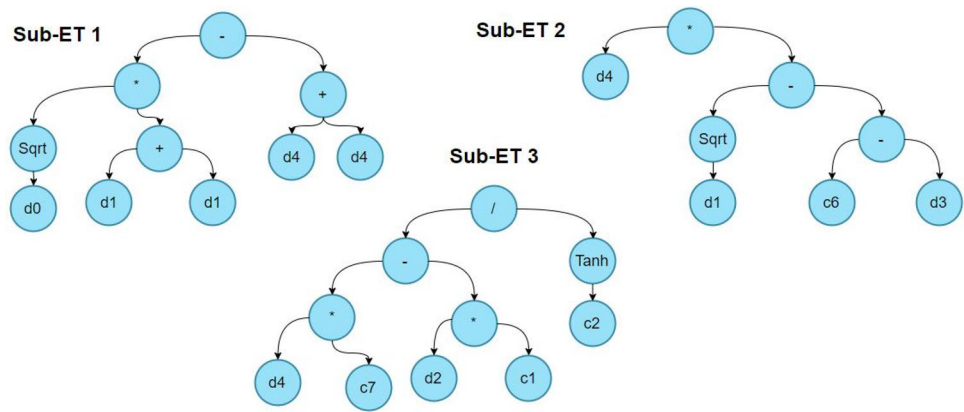


Table 4 Statistical data of Eq. (4)

Description	Training	Testing
Fitness	1.624019	1.646688
MSE	377,925.6	367,575.1
RMSE	614.7565	606.2797
MAE	456.511	457.9939
RSE	8.32E-02	0.145098
RRSE	0.28853	0.380917
RAE	0.310341	0.35956
Correlation coefficient	0.963159	0.968997
R-square	0.927675	0.938955

Table 5 Coefficient of determination results in predicting bearing capacity of CFST columns

Predictive model	R^2	
	Train	Test
ANN	0.895	0.881
PSO-ANN	0.910	0.904
GEP-based Tree	0.928	0.939

section to determine its impact on the performance of models. Figure 14 displays the effects of the most influential parameters on GEP results including the number of generations, the number of genes, and size of head. Therefore, based on Fig. 14, generation, gene, and size of head were considered as 3000, 3, and 5, respectively. Eventually, after the aforementioned implementation, the results of some different models (as equations) are presented in Table 3. This way, different mathematical equations can be compared and their performance can be evaluated for prediction of uniaxial compressive strength in composite columns. In the end, the model No. 4 was chosen as the selected model based on the R^2 results.

According to Fig. 15, the expression tree of each gene of model/ Eq. (4) was presented. All functions and terminal sets were illustrated in the circles. To extract mathematical equations, reading the circles from left to right and top to

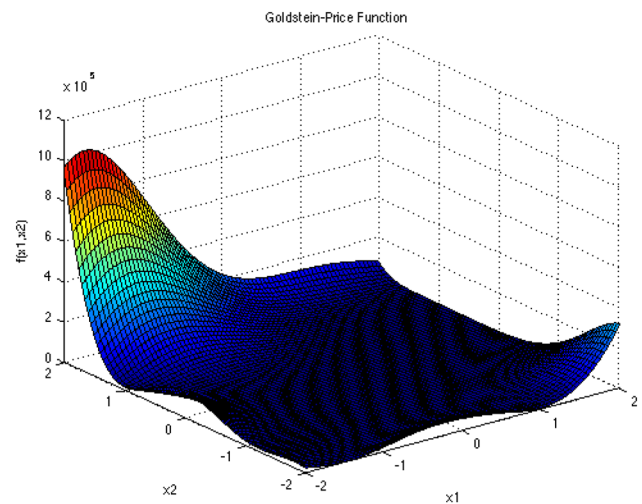


Fig. 16 The three-dimensional graph of Eq. (7)

bottom is recommended (models of 1–5). After extracting the equation of each gene, the final predictive model of GEP was obtained by subtracting of Eq. (4). All statistical data of model No. 4 are presented in Table 4 for both training and testing sections. More discussions regarding the best GEP model will be presented later.

5 Results

Three intelligent systems, i.e., ANN, PSO-ANN, and GEP were developed in this study to predict the bearing capacity of CFST columns. As discussed earlier, many parametric studies were constructed and the best one for each method (ANN, PSO-ANN, and GEP-based tree) was selected. The selection of the best predictive models was based on the results of R^2 . The mentioned results for training and testing datasets of the best predictive models are tabulated in Table 5. According to the obtained results, 0.895 and 0.881 as R^2 of training and testing sections, respectively, are

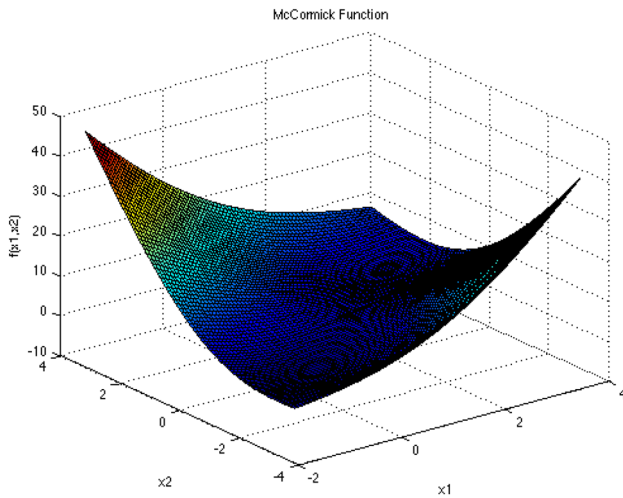


Fig. 17 The three-dimensional graph of Eq. (8)

considered as acceptable finding to estimate bearing capacity of CFST columns. However, if more accurate predictive result is of interest, PSO–ANN can be applied herein. When PSO–ANN model is developed, R^2 results of 0.910 and 0.904 for training and testing datasets can be achieved to estimate bearing capacity of CFST columns. However, if a perfect predictive model (among the applied ones) is of interest, GEP-based tree equation with R^2 values of 0.928 and 0.939 for training and testing datasets has shown its capability. Actually, this technique can provide higher performance capacity compared to other predictive models in estimating bearing capacity of CFST columns. The GEP-based tree can be introduced as a new model that is able to propose new equation for solving problems in structural

engineering fields. In the next section, GEP equation will be used as a cost function for optimizing purposes.

6 Optimization modeling

In this section, the whale optimization algorithm (WOA) is developed to optimize the results of bearing capacity of CFST columns. To examine the WOA algorithm, the selected functions (Eqs. 7, 8) were employed. The minimum values of these functions in the mentioned intervals are 3 and -1.9133 , respectively. Figures 16 and 17 illustrate the three-dimensional graph of these two functions in the specific interval. Figures 18 and 19 demonstrate the results obtained by WOA, which are based on these two equations. As it can be seen, the written code of this algorithm can identify the minimums well. That is why this code can be run for the research conditions obtained in the previous section.

$$F_1(x) = [1 + (x_1 + x_2 + 1)^2(19 - 14x_1 + 3x_1^2 - 14x_2 + 6x_1x_2 + 3x_2^2)] \times [30 + (2x_1 - 3x_2)^2(18 - 32x_1 + 12x_1^2 + 48x_2 - 36x_1x_2 + 27x_2^2)], \tag{7}$$

$$F_2(x) = \sin(x_1 + x_2) + (x_1 + x_2)^2 - 1.5x_1 + 2.5x_2 + 1. \tag{8}$$

To optimize bearing capacity of CFST columns, the selected predictive model (GEP-based tree) was used. In fact, the GEP equation is considered as a cost function in WOA technique. Different models of WOA algorithm (using various parameters) were designed, each of which was executed by adjusting the parameters of the optimization

Fig. 18 The result of WOA algorithm for Eq. (7)

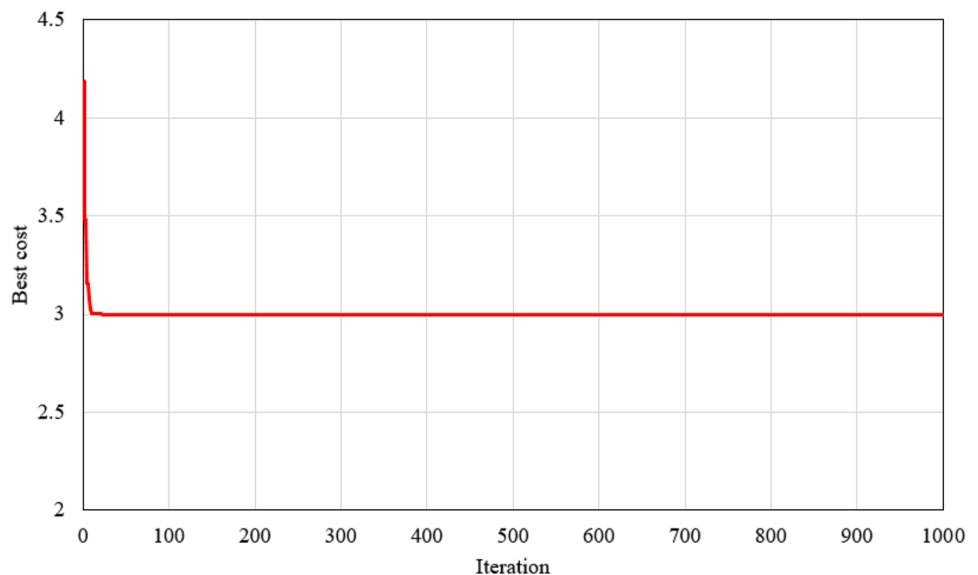


Fig. 19 The result of WOA algorithm for Eq. (8)

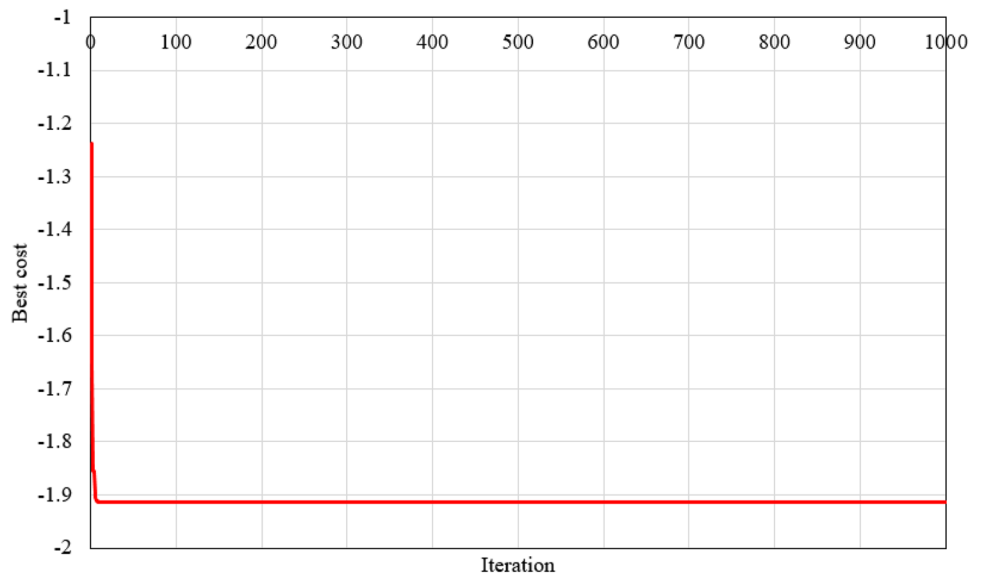


Table 6 The effective parameters of WOA for optimization of the problem

Parameter	Value
Iteration	500
Amounts of search agents	40

algorithm. After a set of conducted analyses, the most appropriate parameters of WOA algorithm were obtained. The best parameters that can deliver well the performance of WOA algorithm for optimizing this problem are presented in Table 6.

With the use of the best model results, the optimum parameters that can provide bearing capacity of CFST columns were determined. The best cost function is presented

in Fig. 20 for this problem. The proposed parameters are given in Table 7. It should be noted that the changes in these parameters are assumed to be the values considered for modeling (Table 1). As it can be seen, in cases where optimization was done, appropriate enhancements were gained in performance of bearing capacity of CFST columns. For example, optimum values of 186.31 MPa, 416.09 mm, 364.31 mm, 6.79 mm, and 823.88 MPa increased the bearing capacity by 23,436.63 kN in comparison with the initial sample. Therefore, different patterns of designing can be applied under various conditions and the best performance can be reached. As a result, WOA is able to optimize the model inputs in a way that maximum amount can be obtained for bearing capacity of CFST columns. As a result,

Fig. 20 The best cost of WOA for optimization of the problem

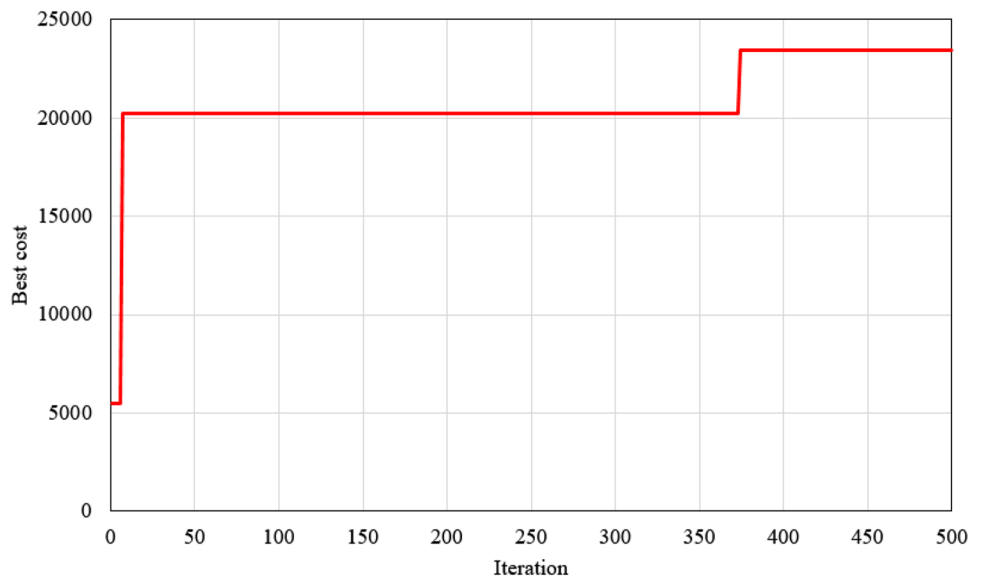


Table 7 The proposed values for optimization of the problem

Parameter	Unit	Optimum value
f'_C	MPa	186.31
D	mm	416.09
L	mm	364.31
t	mm	6.79
f_y	MPa	823.88
Pexp	kN	23,436.63

WOA can be introduced as a powerful optimization algorithm in maximizing bearing capacity of CFST columns.

7 Conclusions

The specification of the bearing capacity of CFST columns made up of hollow steel cylinders filled with concrete is among important issues in constructing different structures. To this end, this paper presented a novel intelligent method to predict and optimize the bearing capacity of such structures. The data used in this research were collected from conducted experimental frameworks. The data comprise parameters of the outer diameter, concrete compressive strength, tensile yield stress of the steel column, steel cover thickness, and length of the used samples. The ANN and neuro-swarm methods were used for prediction purposes. The GEP-based tree model was implemented and developed under different conditions to predict the bearing capacity of CFST columns and finally, an equation was proposed to estimate bearing capacity of CFST columns. Based on the obtained results, the GEP-based tree equation with R^2 values of 0.928 and 0.939 for training and testing datasets, respectively, indicates higher performance capacity compared to ANN and neuro-swarm predictive models. On the other hand, neuro-swarm provided higher performance capacity compared to ANN. Therefore, the GEP-based tree technique was selected as the best predictive model for estimating the bearing capacity of CFST columns. A GEP-based tree equation was used as a cost function in the WOA optimization algorithm. Different WOA models were constructed to obtain higher values of the bearing capacity. According to the obtained results, it was found that WOA (with increasing bearing capacity to 23436.63 kN) was able to maximize significantly the bearing capacity of the CFST columns. The optimum values obtained in this study allow engineers and researchers to reach the best performance in designing and constructing CFST columns.

References

- Lai MH, Ho JCM (2015) Effect of continuous spirals on uniaxial strength and ductility of CFST columns. *J Constr Steel Res* 104:235–249
- Elbaz K, Shen S-L, Zhou A et al (2019) Optimization of EPB shield performance with adaptive neuro-fuzzy inference system and genetic algorithm. *Appl Sci* 9:780
- Lyu H-M, Shen S-L, Zhou A, Yang J (2019) Perspectives for flood risk assessment and management for mega-city metro system. *Tunn Undergr Sp Technol* 84:31–44
- Liu X, Shen S, Zhou A, Xu Y (2019) Evaluation of foam conditioning effect on groundwater inflow at tunnel cutting face. *Int J Numer Anal Methods Geomech* 43:463–481
- Yu Z, Ding F, Cai CS (2007) Experimental behavior of circular concrete-filled steel tube stub columns. *J Constr Steel Res* 63:165–174
- Beheshti-Aval SB (2012) Strength evaluation of concrete-filled steel tubes subjected to axial-flexural loading by ACI and AISC-LRFD codes along with three dimensional nonlinear analysis. *Int J Civ Eng* 10:280–290
- Perea T, Leon RT, Hajjar JF, Denavit MD (2014) Full-scale tests of slender concrete-filled tubes: interaction behavior. *J Struct Eng* 140:4014054
- Ahmadi M, Naderpour H, Kheyroddin A (2017) ANN model for predicting the compressive strength of circular steel-confined concrete. *Int J Civ Eng* 15:213–221
- He L, Zhao Y, Lin S (2018) Experimental study on axially compressed circular CFST columns with improved confinement effect. *J Constr Steel Res* 140:74–81
- Shams S, Monjezi M, Majd VJ, Armaghani DJ (2015) Application of fuzzy inference system for prediction of rock fragmentation induced by blasting. *Arab J Geosci* 8:10819–10832
- Armaghani DJ, Hajihassani M, Sohaei H et al (2015) Neuro-fuzzy technique to predict air-overpressure induced by blasting. *Arab J Geosci* 8:10937–10950. <https://doi.org/10.1007/s12517-015-1984-3>
- Zhao Y, Noorbakhsh A, Koopialipour M et al (2019) A new methodology for optimization and prediction of rate of penetration during drilling operations. *Eng Comput*. <https://doi.org/10.1007/s00366-019-00715-2>
- Koopialipour M, Fahimifar A, Ghaleini EN et al (2019) Development of a new hybrid ANN for solving a geotechnical problem related to tunnel boring machine performance. *Eng Comput*. <https://doi.org/10.1007/s00366-019-00701-8>
- Koopialipour M, Murlidhar BR, Hedayat A et al (2019) The use of new intelligent techniques in designing retaining walls. *Eng Comput*. <https://doi.org/10.1007/s00366-018-00700-1>
- Koopialipour M, Nikouei SS, Marto A et al (2018) Predicting tunnel boring machine performance through a new model based on the group method of data handling. *Bull Eng Geol Environ* 208:1–15
- Zhou J, Shi X, Li X (2016) Utilizing gradient boosted machine for the prediction of damage to residential structures owing to blasting vibrations of open pit mining. *J Vib Control* 22:3986–3997
- Zhou J, Shi X, Du K et al (2016) Feasibility of random-forest approach for prediction of ground settlements induced by the construction of a shield-driven tunnel. *Int J Geomech* 17:4016129
- Zhou J, Li X, Mitri HS (2016) Classification of rockburst in underground projects: comparison of ten supervised learning methods. *J Comput Civ Eng* 30:4016003
- Wang M, Shi X, Zhou J, Qiu X (2018) Multi-planar detection optimization algorithm for the interval charging structure of large-diameter longhole blasting design based on rock fragmentation aspects. *Eng Optim* 50:2177–2191
- Asteris PG, Plevris V (2017) Anisotropic masonry failure criterion using artificial neural networks. *Neural Comput Appl* 28:2207–2229
- Asteris PG, Tsaris AK, Cavaleri L et al (2016) Prediction of the fundamental period of infilled RC frame structures using artificial neural networks. *Comput Intell Neurosci* 2016:20

22. Asteris PG, Nikoo M (2019) Artificial bee colony-based neural network for the prediction of the fundamental period of infilled frame structures. *Neural Comput Appl*. <https://doi.org/10.1007/s00521-018-03965-1>
23. Armaghani DJ, Koopialipoor M, Marto A, Yagiz S (2019) Application of several optimization techniques for estimating TBM advance rate in granitic rocks. *J Rock Mech Geotech Eng*. <https://doi.org/10.1016/j.jrmge.2019.01.002>
24. Koopialipoor M, Tootoonchi H, Jahed Armaghani D et al (2019) Application of deep neural networks in predicting the penetration rate of tunnel boring machines. *Bull Eng Geol Environ*. <https://doi.org/10.1007/s10064-019-01538-7>
25. Zhou J, Aghili N, Ghaleini EN et al (2019) A Monte Carlo simulation approach for effective assessment of flyrock based on intelligent system of neural network. *Eng Comput*. <https://doi.org/10.1007/s00366-019-00726-z>
26. Koopialipoor M, Ghaleini EN, Tootoonchi H et al (2019) Developing a new intelligent technique to predict overbreak in tunnels using an artificial bee colony-based ANN. *Environ Earth Sci* 78:165. <https://doi.org/10.1007/s12665-019-8163-x>
27. Liao X, Khandelwal M, Yang H et al (2019) Effects of a proper feature selection on prediction and optimization of drilling rate using intelligent techniques. *Eng Comput*. <https://doi.org/10.1007/s00366-019-00711-6>
28. Zhou J, Li X, Mitri HS (2018) Evaluation method of rockburst: state-of-the-art literature review. *Tunn Undergr Sp Technol* 81:632–659
29. Zhou J, Li X, Shi X (2012) Long-term prediction model of rockburst in underground openings using heuristic algorithms and support vector machines. *Saf Sci* 50:629–644
30. Armaghani DJ, Hasanipanah M, Amnieh HB, Mohamad ET (2018) Feasibility of ICA in approximating ground vibration resulting from mine blasting. *Neural Comput Appl* 29:457–465
31. Rabunal JR, Puertas J (2006) Hybrid system with artificial neural networks and evolutionary computation in civil engineering. *Artificial Neural Networks in real-life applications*. IGI Global, Pennsylvania, pp 166–187
32. Ni H-G, Wang J-Z (2000) Prediction of compressive strength of concrete by neural networks. *Cem Concr Res* 30:1245–1250
33. Toghroli A, Mohammadhassani M, Suhatri M et al (2014) Prediction of shear capacity of channel shear connectors using the ANFIS model. *Steel Compos Struct* 17:623–639
34. Lee S-C (2003) Prediction of concrete strength using artificial neural networks. *Eng Struct* 25:849–857
35. Naderpour H, Kheyroddin A, Amiri GG (2010) Prediction of FRP-confined compressive strength of concrete using artificial neural networks. *Compos Struct* 92:2817–2829
36. Asteris PG, Kolovos KG (2019) Self-compacting concrete strength prediction using surrogate models. *Neural Comput Appl* 31:409–424
37. Asteris PG, Nozhati S, Nikoo M et al (2018) Krill herd algorithm-based neural network in structural seismic reliability evaluation. *Mech Adv Mater Struct* 2018:1–8
38. Asteris P, Roussis P, Douvika M (2017) Feed-forward neural network prediction of the mechanical properties of sandcrete materials. *Sensors* 17:1344
39. Toghroli A, Suhatri M, Ibrahim Z et al (2018) Potential of soft computing approach for evaluating the factors affecting the capacity of steel–concrete composite beam. *J Intell Manuf* 29:1793–1801
40. Safa M, Shariati M, Ibrahim Z et al (2016) Potential of adaptive neuro fuzzy inference system for evaluating the factors affecting steel–concrete composite beam's shear strength. *Steel Compos Struct* 21:679–688
41. Effati M, Rajabi MA, Samadzadegan F, Shabani S (2014) A geospatial based neuro-fuzzy modeling for regional transportation corridors hazardous zones identification. *Int J Civ Eng* 2014:12
42. Kaveh A, Maniat M (2014) Damage detection in skeletal structures based on charged system search optimization using incomplete modal data. *Int J Civ Eng IUST* 12:291–298
43. Kaveh A, Ghaffarian R (2015) Shape optimization of arch dams with frequency constraints by enhanced charged system search algorithm and neural network. *Int J Civ Eng* 13:102–111
44. Eberhart R, Simpson P, Dobbins R (1996) *Computational intelligence PC tools*. Academic Press Prof Inc, London
45. Faradonbeh RS, Hasanipanah M, Amnieh HB et al (2018) Development of GP and GEP models to estimate an environmental issue induced by blasting operation. *Environ Monit Assess* 190:351
46. Faradonbeh RS, Jahed Armaghani D, Monjezi M (2016) Development of a new model for predicting flyrock distance in quarry blasting: a genetic programming technique. *Bull Eng Geol Environ*. <https://doi.org/10.1007/s10064-016-0872-8>
47. Shirani Faradonbeh R, Jahed Armaghani D, Abd Majid MZ et al (2016) Prediction of ground vibration due to quarry blasting based on gene expression programming: a new model for peak particle velocity prediction. *Int J Environ Sci Technol*. <https://doi.org/10.1007/s13762-016-0979-2>
48. Faradonbeh RS, Armaghani DJ, Monjezi M, Mohamad ET (2016) Genetic programming and gene expression programming for flyrock assessment due to mine blasting. *Int J Rock Mech Min Sci* 88:254–264
49. Armaghani DJ, Faradonbeh RS, Rezaei H et al (2016) Settlement prediction of the rock-socketed piles through a new technique based on gene expression programming. *Neural Comput Appl*. <https://doi.org/10.1007/s00521-016-2618-8>
50. Jahed Armaghani D, Faradonbeh RS, Momeni E et al (2017) Performance prediction of tunnel boring machine through developing a gene expression programming equation. *Eng Comput*. <https://doi.org/10.1007/s00366-017-0526-x>
51. Armaghani DJ, Safari V, Fahimifar A et al (2017) Uniaxial compressive strength prediction through a new technique based on gene expression programming. *Neural Comput Appl* 2017:1–10
52. Saad S, Malik H (2018) Gene expression programming (GEP) based intelligent model for high performance concrete comprehensive strength analysis. *J Intell Fuzzy Syst* 2018:1–16
53. Aval SBB, Ketabdari H, Gharebaghi SA (2017) Estimating shear strength of short rectangular reinforced concrete columns using nonlinear regression and gene expression programming. *Structures*. Elsevier, Oxford, pp 13–23
54. Yi LU, Xiangyun LUO, Zhang H (2011) A gene expression programming algorithm for highway construction cost prediction problems. *J Transp Syst Eng Inf Technol* 11:85–92
55. Azamathulla HM (2013) Gene-expression programming to predict friction factor for Southern Italian rivers. *Neural Comput Appl* 23:1421–1426
56. Azamathulla HM, Cuan YC, Ghani AA, Chang CK (2013) Suspended sediment load prediction of river systems: GEP approach. *Arab J Geosci* 6:3469–3480
57. Hebb DO (1955) Drives and the CNS (conceptual nervous system). *Psychol Rev* 62:243
58. Momeni E, Nazir R, Armaghani DJ, Maizir H (2015) Application of artificial neural network for predicting shaft and tip resistances of concrete piles. *Earth Sci Res J* 19:85–93
59. Mohamad ET, Armaghani DJ, Hajihassani M et al (2013) A simulation approach to predict blasting-induced flyrock and size of thrown rocks. *Electron J Geotech Eng* 18 B:365–374
60. Jahed Armaghani D, Tonnizam Mohamad E, Hajihassani M et al (2016) Evaluation and prediction of flyrock resulting from blasting operations using empirical and computational methods. *Eng Comput*. <https://doi.org/10.1007/s00366-015-0402-5>

61. Koopialipour M, Armaghani DJ, Hedayat A et al (2018) Applying various hybrid intelligent systems to evaluate and predict slope stability under static and dynamic conditions. *Soft Comput.* <https://doi.org/10.1007/s00500-018-3253-3>
62. Koopialipour M, Armaghani DJ, Haghighi M, Ghaleini EN (2017) A neuro-genetic predictive model to approximate overbreak induced by drilling and blasting operation in tunnels. *Bull Eng Geol Environ.* <https://doi.org/10.1007/s10064-017-1116-2>
63. Koopialipour M, Ghaleini EN, Haghighi M et al (2018) Overbreak prediction and optimization in tunnel using neural network and bee colony techniques. *Eng Comput* 1:4. <https://doi.org/10.1007/s00366-018-0658-7>
64. Mohamad ET, Faradonbeh RS, Armaghani DJ et al (2017) An optimized ANN model based on genetic algorithm for predicting ripping production. *Neural Comput Appl* 28:393–406
65. Kennedy J, Eberhart RC (1995) A discrete binary version of the particle swarm algorithm. In: *Systems, man, and cybernetics, 1997. Computational cybernetics and simulation. 1997 IEEE international conference on IEEE*, pp 4104–4108
66. Jahed Armaghani D, Hajihassani M, Yazdani Bejarbaneh B et al (2014) Indirect measure of shale shear strength parameters by means of rock index tests through an optimized artificial neural network. *Meas J Int Meas Confed.* <https://doi.org/10.1016/j.measurement.2014.06.001>
67. Koopialipour M, Fallah A, Armaghani DJ et al (2018) Three hybrid intelligent models in estimating flyrock distance resulting from blasting. *Eng Comput.* <https://doi.org/10.1007/s00366-018-0596-4>
68. Gordan B, Jahed Armaghani D, Hajihassani M, Monjezi M (2016) Prediction of seismic slope stability through combination of particle swarm optimization and neural network. *Eng Comput.* <https://doi.org/10.1007/s00366-015-0400-7>
69. Ferreira C (2001) Algorithm for solving gene expression programming: a new adaptive problems. *Complex Syst* 13:87–129
70. Khandelwal M, Armaghani DJ, Faradonbeh RS et al (2016) A new model based on gene expression programming to estimate air flow in a single rock joint. *Environ Earth Sci* 75:739
71. Keshavarz A, Mehramiri M (2015) New Gene Expression Programming models for normalized shear modulus and damping ratio of sands. *Eng Appl Artif Intell* 45:464–472
72. Khandelwal M, Faradonbeh RS, Monjezi M et al (2017) Function development for appraising brittleness of intact rocks using genetic programming and non-linear multiple regression models. *Eng Comput* 33:13–21
73. Ferreira C (2006) *Gene expression programming: mathematical modeling by an artificial intelligence.* Springer, Berlin
74. Mirjalili S, Lewis A (2016) The whale optimization algorithm. *Adv Eng Softw* 95:51–67
75. Watkins WA, Schevill WE (1979) Aerial observation of feeding behavior in four baleen whales: *Eubalaena glacialis*, *Balaenoptera borealis*, *Megaptera novaeangliae*, and *Balaenoptera physalus*. *J Mammal* 60:155–163
76. Goldbogen JA, Friedlaender AS, Calambokidis J et al (2013) Integrative approaches to the study of baleen whale diving behavior, feeding performance, and foraging ecology. *Bioscience* 63:90–100
77. Le Hoang A, Fehling E (2017) Numerical study of circular steel tube confined concrete (STCC) stub columns. *J Constr Steel Res* 136:238–255
78. Le Hoang A, Fehling E, Thai D-K, Van Nguyen C (2019) Evaluation of axial strength in circular STCC columns using UHPC and UHPFRC. *J Constr Steel Res* 153:533–549
79. Giakoumelis G, Lam D (2004) Axial capacity of circular concrete-filled tube columns. *J Constr Steel Res* 60:1049–1068
80. Sakino K, Nakahara H, Morino S, Nishiyama I (2004) Behavior of centrally loaded concrete-filled steel-tube short columns. *J Struct Eng* 130:180–188
81. Zeghiche J, Chaoui K (2005) An experimental behaviour of concrete-filled steel tubular columns. *J Constr Steel Res* 61:53–66
82. Han L-H, Yao G-H (2003) Behaviour of concrete-filled hollow structural steel (HSS) columns with pre-load on the steel tubes. *J Constr Steel Res* 59:1455–1475
83. O'Shea MD, Bridge RQ (2000) Design of circular thin-walled concrete filled steel tubes. *J Struct Eng* 126:1295–1303
84. Khandelwal M, Armaghani DJ (2016) Prediction of drillability of rocks with strength properties using a hybrid GA-ANN technique. *Geotech Geol Eng* 34:605–620. <https://doi.org/10.1007/s10706-015-9970-9>
85. Khandelwal M, Kumar DL, Yellishetty M (2011) Application of soft computing to predict blast-induced ground vibration. *Eng Comput* 27:117–125
86. Ghaleini EN, Koopialipour M, Momenzadeh M et al (2018) A combination of artificial bee colony and neural network for approximating the safety factor of retaining walls. *Eng Comput* 35:647. <https://doi.org/10.1007/s00366-018-0625-3>
87. Gordan B, Koopialipour M, Clementking A et al (2018) Estimating and optimizing safety factors of retaining wall through neural network and bee colony techniques. *Eng Comput.* <https://doi.org/10.1007/s00366-018-0642-2>
88. Koopialipour M, Noorbakhsh A, Noroozi Ghaleini E et al (2019) A new approach for estimation of rock brittleness based on non-destructive tests. *Nondestruct Test Eval* 2019:1–22. <https://doi.org/10.1080/10589759.2019.1623214>
89. Khandelwal M, Mahdiyar A, Armaghani DJ et al (2017) An expert system based on hybrid ICA-ANN technique to estimate macerals contents of Indian coals. *Environ Earth Sci* 76:399. <https://doi.org/10.1007/s12665-017-6726-2>
90. Hajihassani M, Jahed Armaghani D, Monjezi M et al (2015) Blast-induced air and ground vibration prediction: a particle swarm optimization-based artificial neural network approach. *Environ Earth Sci.* <https://doi.org/10.1007/s12665-015-4274-1>
91. Bunawan AR, Momeni E, Armaghani DJ, Rashid ASA (2018) Experimental and intelligent techniques to estimate bearing capacity of cohesive soft soils reinforced with soil-cement columns. *Measurement* 124:529–538
92. Mahdiyar A, Armaghani DJ, Marto A et al (2018) Rock tensile strength prediction using empirical and soft computing approaches. *Bull Eng Geol Environ.* <https://doi.org/10.1007/s10064-018-1405-4>
93. Armaghani DJ, Mohamad ET, Narayanasamy MS et al (2017) Development of hybrid intelligent models for predicting TBM penetration rate in hard rock condition. *Tunn Undergr Sp Technol* 63:29–43. <https://doi.org/10.1016/j.tust.2016.12.009>
94. Brownlee J (2011) *Clever algorithms: nature-inspired programming recipes.* Jason Brownlee

Publisher's Note Springer Nature remains neutral with regard to jurisdictional claims in published maps and institutional affiliations.

Affiliations

Payam Sarir¹ · Jun Chen¹ · Panagiotis G. Asteris² · Danial Jahed Armaghani³ · M. M. Tahir⁴

Payam Sarir
p.sarir@sjtu.edu.cn

Panagiotis G. Asteris
asteris@aspete.gr

M. M. Tahir
mahmoodtahir@utm.my

¹ State Key Laboratory of Ocean Engineering, School of Naval Architecture, Ocean, and Civil Engineering, Shanghai Jiao Tong University, Shanghai 200240, China

² Computational Mechanics Laboratory, School of Pedagogical and Technological Education, Heraklion, 14121 Athens, Greece

³ Institute of Research and Development, Duy Tan University, Da Nang 550000, Vietnam

⁴ UTM Construction Research Centre, Institute for Smart Infrastructure and Innovative Construction (ISIIC), School of Civil Engineering, Faculty of Engineering, Universiti Teknologi Malaysia, 81310 Johor Bahru, Johor, Malaysia